Article

Adsorption and Mechanism of Glycine on the Anatase with Exposed (001) and (101) Facets

Zeling Liu [1], Xiaomei Zhong [1], Yifan Liu [1], Hanyun Rao [1], Hongfu Wei [1], Wenyuan Hu [2], Xiaoqin Nie [3] and Mingxue Liu [1,*]

[1] School of Life Science and Engineering, Southwest University of Science and Technology, Mianyang 621010, China; liuzeling1998@163.com (Z.L.); zhongxiaomei_swust@163.com (X.Z.); yifanliuswust@163.com (Y.L.); hanyun_rao@163.com (H.R.); weihongfu@swust.edu.cn (H.W.)
[2] School of Material Science and Engineering, Southwest University of Science and Technology, Mianyang 621010, China; huwenyuan@swust.edu.cn
[3] School of National Defense Science and Technology, Southwest University of Science and Technology, Mianyang 621010, China; xiaoqin_nie@163.com
* Correspondence: liumingxue@swust.edu.cn; Tel.: +86-13-550-832-055

Abstract: As a widely existing mineral types on Earth, semiconductor minerals play an important role in the origin of life and the material geochemical cycle. The first step of peptide formation is amino acid adsorption on the mineral surface, but the role and mechanism of different crystal facets of semiconductor minerals are not well understood. Anatase (TiO_2) with exposed (001) facets was synthesized by a hydrothermal method, and then analyzed and compared with the purchased ordinary anatase (TiO_2) for the adsorption of glycine, the simplest amino acid. XRD, SEM and TEM results show that the hydrothermally synthesized anatase (TiO_2) has a good anatase crystal form, which is micro-nano-scale flake particles and mainly composed of (001) facets. The results of HPLC used in the adsorption experiment showed that under optimal conditions (pH 5 to 6, an adsorption time of 24 h, and an initial concentration of 0.09 mol/L), the adsorption quantity of glycine on anatase (TiO_2) with exposed (001) facets may reach 10 mg/m^2, which is larger than that for ordinary anatase (TiO_2) with exposed (101) facets. Based on a combination of various characterizations and simulation calculations, the results proved that anatase can activate thermodynamically stable γ-glycine to β-glycine. The adsorption of glycine on anatase (TiO_2) has two forms, one is the zwitterionic form in which the carboxyl group forms a bridge structure with two Ti atoms connected by surface bridging oxygen, and the dissociated form is in which the amino group forms a bond with the surface Ti atom. Among these, glycine is mainly adsorbed to anatase by dissociative molecules on the anatase (TiO_2) with exposed (001) facets and by zwitterion adsorption on the anatase (TiO_2) with exposed (101) facets. This research elucidates the conditions and mechanism of amino acid adsorption by semiconductor minerals in weak acidic environment, which is similar to the environmental pH that was beneficial to the formation of life on the early Earth. Therefore, these can provide a reference for the further study of the role of semiconductor minerals in the adsorption and polymerization of small biomolecules in the origin of life.

Keywords: anatase (TiO_2); facet; glycine; adsorption; mechanism; simulation calculation

1. Introduction

Many biological and biogeochemical processes such as biomedical implant devices, biomineralization, and prebiotic chemistry, as well as the origin and early evolution of life, may be attributed to the interaction between biomolecules and mineral surfaces [1,2]. In 1951, Bernal proposed the hypothesis that life originated from the adsorption of organic molecules on clay, which paved the way for a series of experiments on the adsorption of small biomolecules and polymerization on the surface of clay minerals [3]. All processes of life are inseparable from the participation of proteins, in which the initial step includes the

adsorption of amino acids and polymerization into peptides catalyzed by many minerals [4]. Many researchers use the interaction between clay minerals and amino acids to explore the evolution of early biological macromolecules, but the mechanism of action is still unclear. Many clays, such as montmorillonite [5–8], kaolinite [2,9], and hectorite [10], and some oxide/oxyhydroxide minerals such as γ-Al_2O_3 [1,11], goethite (α-FeOOH) [12], etc., were measured for the adsorption and polymerization of amino acids. However, most previous studies have focused on the adsorption of amino acids with negatively and positively charged side chains on the hydroxyl surface, such as glutamic acid, aspartic acid, and lysine. Few studies have been carried out on the adsorption of amino acids with neutrally charged side chains or carboxylic acids with only a single carboxyl group, such as glycine [1]. It has been reported that the active groups of amino acids are mainly adsorbed to clay or oxides through electrostatic attraction, hydrophobic interaction, covalent bonding, and hydrogen bonding [13,14]. Tentorio and Canova [15] showed that L-glutamic acid and L-(+)-lysine are adsorbed on amorphous Ti hydrous oxide through hydrogen bonding between deprotonated amino groups and surface hydroxyl groups when electrostatic repulsion prevails.

The photoelectrons generated by the catalysis of semiconductor minerals under various conditions played a variety of roles in the evolution of life on Earth, such as synthesizing substances, protecting cells and providing energy [16]. Understanding the interactions of amino acids with mineral surfaces is important for better understanding biocomponent surface interactions and the role of mineral surfaces in the origin of life on Earth [17,18]. Amino acids have the characteristic of adsorbing anions, which have amide or aromatic side chains have weaker interactions with titanium dioxide due to their lack of acidic side chains [19,20]. Roddick and McQuillan [21] used in situ ATR-IR spectroscopy to study the molecular structure of glutamic acid and aspartic acid adsorbed on amorphous titanium dioxide for the first time, and found that small changes in the chemical structure of amino acids can significantly affect the adsorption behavior of titanium dioxide. By establishing and calculating theoretical models, it is helpful to understand the adsorption behavior on the substrate surface [19]. When in a neutral pH environment, water molecules can be adsorbed on the surface of gibbsite through hydrogen bonding [22]. Ferrante et al. [23] calculated by density functional theory that the adsorption capacity of carboxyl groups on the halloysite surface is stronger than that of alcohol groups and halides. The carboxyl groups of organic acids such as formic acid and acetic acid are strongly adsorbed on the surface of rutile by bridge coordination [24]. When using first-principles calculations for the interaction of glycine with anatase (101) surface, the researchers found that the carboxyl group of glycine exhibits a stronger binding energy than formic acid [25].

Natural semiconductor minerals include metal sulfides and metal oxides, in which the metal oxide band gap is often greater than 1.5 eV [16]. Anatase (TiO_2) has attracted a lot of attention because of its low cost, non-toxic and good photocatalytic performance, which can be used as a model mineral [26,27]. It is widely used in the degradation of organic pollutants [28], heavy metals [29], dye-sensitized solar cells [26], biomedical fields [27]. However, anatase (TiO_2) particles have defects such as low utilization of visible light and easy recombination of photogenerated electrons and holes [30]. With improvements in synthesis technology and further study of the crystal structure of anatase (TiO_2), theoretical and experimental studies have shown that anatase (TiO_2) with exposed (001) facets has high photocatalytic activity [31]. In general, ordinary anatase is composed of (101) crystal facets with higher surface energy, while (001) crystal facets with higher reactivity are almost non-existent due to their low surface energy. Yang et al. [32] used fluoride compounds as control agents to synthesize anatase (TiO_2) with both (001) crystal faces and (101) crystal facets, which opened up a new journey for the synthesis of crystal facets with high reactivity. Since then, much research has been carried out on synthetic anatase (TiO_2) with exposed (001) facets, and the crystal facet exposure rate has been continuously improved, which has now reached about 80% now [33]. However, most research has focused on the adsorption of amino acids on TiO_2 with (110) single-crystal facets [34–37]. It was found that the

(001) surface is more active than most surfaces and plays a key role in the reactivity of anatase nanoparticles [38]. There are few comparative studies for adsorption of amino acids on minerals with different crystal faces, the roles and mechanisms semiconductor minerals with different crystal facets on adsorption of amino acids are still unclear. In view of the important roles of semiconducting minerals and amino acids in the origin of life, we combined experimental and simulation work to discuss the adsorption mechanism of glycine on anatase (TiO_2). The purpose is to explore the interfacial effect of two crystal facets of anatase (TiO_2) on adsorption of amino acids, and to provide a reference for exploring the evolution of biological molecules in the process of life origin.

Therefore, studying the adsorption behavior and mechanism of amino acids on semiconductor minerals is very important for clarifying the related reactions between semiconductor minerals and amino acid molecules in the evolution of life. In this research, anatase (TiO_2) with exposed (001) facets was synthesized by a hydrothermal method. Through the adsorption of glycine by anatase (TiO_2) with two different crystal facets, the synthesis and reaction products were characterized by SEM, TEM, XRD, HPLC, Raman spectroscopy, and XPS. Finally, the adsorption mechanism of anatase (TiO_2) was simulated by using Material Studio software to explore the interface effect and mechanism of anatase (TiO_2) with two different crystal facets on organic molecules.

2. Materials and Methods

2.1. Sample Preparation

Ordinary anatase (TiO_2) samples were purchased from Shijiazhuang Yunpo Chemical Co. Ltd., and the method described by Feng et al. [39] was used to synthesize anatase (TiO_2) with exposed (001) facets. Firstly, 2.0 mL of tetrabutyl titanate and 0.5–1.0 g of ammonium hexafluorotitanate $(NH_4)_2TiF_6$ was added into a 50% hydrochloric acid solution. After the solution had been poured into a stainless steel autoclave, it was reacted for 24 h at 180 °C in muffle furnace. Finally, after centrifugation and drying, the product was placed in a muffle furnace and heated to 400–500 °C for 2 h to remove fluorine atoms.

An X-ray diffractometer (PANalytical, X'pert PRO Netherlands) was used to obtain XRD spectra of the two kinds of anatase (TiO_2). An Ultra55 high-resolution cold field emission scanning electron microscope (SEM) from Carl Zeiss NTS GmbH, Germany, and a JEOL-2010 high-resolution transmission electron microscope from JEOL Ltd. were used to observe the morphology and structure of the anatase samples.

2.2. Adsorption Experiment

The factors investigated were the pH, adsorption time, and glycine concentration. Firstly, after mixing glycine with anatase (TiO_2) for a period of time, the sample was separated at 6796× g for 10 min. Next, the supernatant was filtered with a 0.45 μm microporous membrane, and the concentration of the solution was measured by HPLC. The pellet after centrifugation was dried and characterized by Raman spectroscopy and XPS.

The HPLC mobile phase was prepared as follows: 0.941 g of sodium hexane sulfonate was dissolved in 500 mL of ultrapure water, and the pH was adjusted to 2.5 with H_3PO_4. After suction filtration with a 0.45 μm microporous membrane and an ultrasonic exhaust, the solution could be used as a mobile phase. The test conditions were as follows: a flow rate of 0.6 mL/min, a sodium hexanesulfonate/acetonitrile ratio of 95:5, a temperature of 30 °C, an absorption wavelength of 200 nm, and an injection volume of 50 μL. The adsorption capacity of glycine was determined by the external standard single-point method.

The Raman spectra were measured with an INVIA laser Raman spectrometer produced by Renishaw, London, UK, and a Thermo Escalab 250Xi X-ray photoelectron spectrometer produced by Thermoelectricity, Waltham, Massachusetts, US, was used for XPS analysis.

2.3. Simulation Calculation

Material Studio software was used to simulate the adsorption of glycine on the anatase (TiO_2) with exposed (001) facets and the anatase (TiO_2) with exposed (101) facets. The

CASTEP module in the software completes the structure optimization and energy calculation of the whole process. The exchange correlation between electrons was described by the PEB function under the generalized gradient (GGA). The cutoff energy of the plane wave was set as 300 eV, the first Brillouin region was divided into $2 \times 2 \times 2$ grids, and the energy convergence standard was set as 2.0 to 5.0 eV/atom. The adsorption energy calculation formula was [40]:

$$E_{ads} = E_{(slab-molecule)} - (E_{molecule} + E_{slab}) \tag{1}$$

where E_{ads} is the adsorption energy of a glycine molecule on the surface, $E_{(slab-molecule)}$ is the total energy of the glycine molecule adsorbed on the crystal facets, $E_{molecule}$ is the total molecular energy of glycine, and E_{slab} is the total energy of the crystal facets.

3. Results and Discussion

3.1. Synthesis of Anatase (TiO$_2$) with Exposed (001) Facets and Characterization of the Sample

Figure 1 shows the XRD spectra of anatase (TiO$_2$) with two different crystal facets. The dominant planes of anatase (TiO$_2$) are the (101), (001), (010), and (100) planes, of which the (101) facets is the most common [41]. The two kinds of anatase (TiO$_2$) were consistent with the standard PDF cards in the Jade 6.0 search database (JCPDS No. 99-0008); both are standard anatase (TiO$_2$). Compared with the anatase (TiO$_2$) that had been purchased, the intensity of each diffraction peak of the anatase (TiO$_2$) with exposed (001) facets increased significantly, and it had a better and more complete anatase crystal form [42]. In addition to the (101) facets' diffraction peak, the diffraction peak of the (004) facets also increased significantly, indicating that the synthesized anatase (TiO$_2$) nanoparticles mainly developed along the [001] direction [43]. The diffraction peaks that usually exist in some single crystals or polycrystals disappeared, indicating that these solids are highly oriented, leading to the absence of diffraction peaks of (001) crystal facets in the XRD spectrum [39]. The results are consistent with the patterns of anatase (TiO$_2$) synthesized by various methods [44,45].
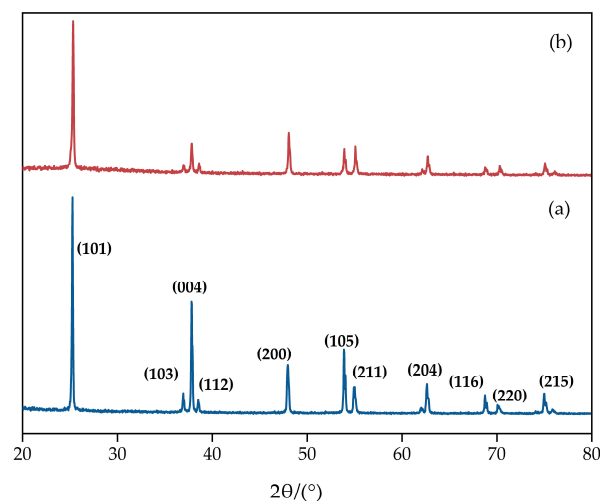

Figure 1. XRD diagram of anatase (TiO$_2$) with exposed (001) facets (**a**) and anatase (TiO$_2$) with exposed (101) facets (**b**).

Compared with anatase (TiO$_2$) with exposed (001) facets which had a nano-sized spindle-shaped pyramid structure, anatase (TiO$_2$) with exposed (001) facets had micro-nano flaky particles and had a larger exposed surface (Figure 2). The synthesized crystal was thin and uniform in size, and its morphology was consistent with the literature. Because of the influence of the synthesis method, the number of raw materials, the experimental temperature, etc., the synthesized anatase (TiO$_2$) in this study is thinner than that found in the literature [46].
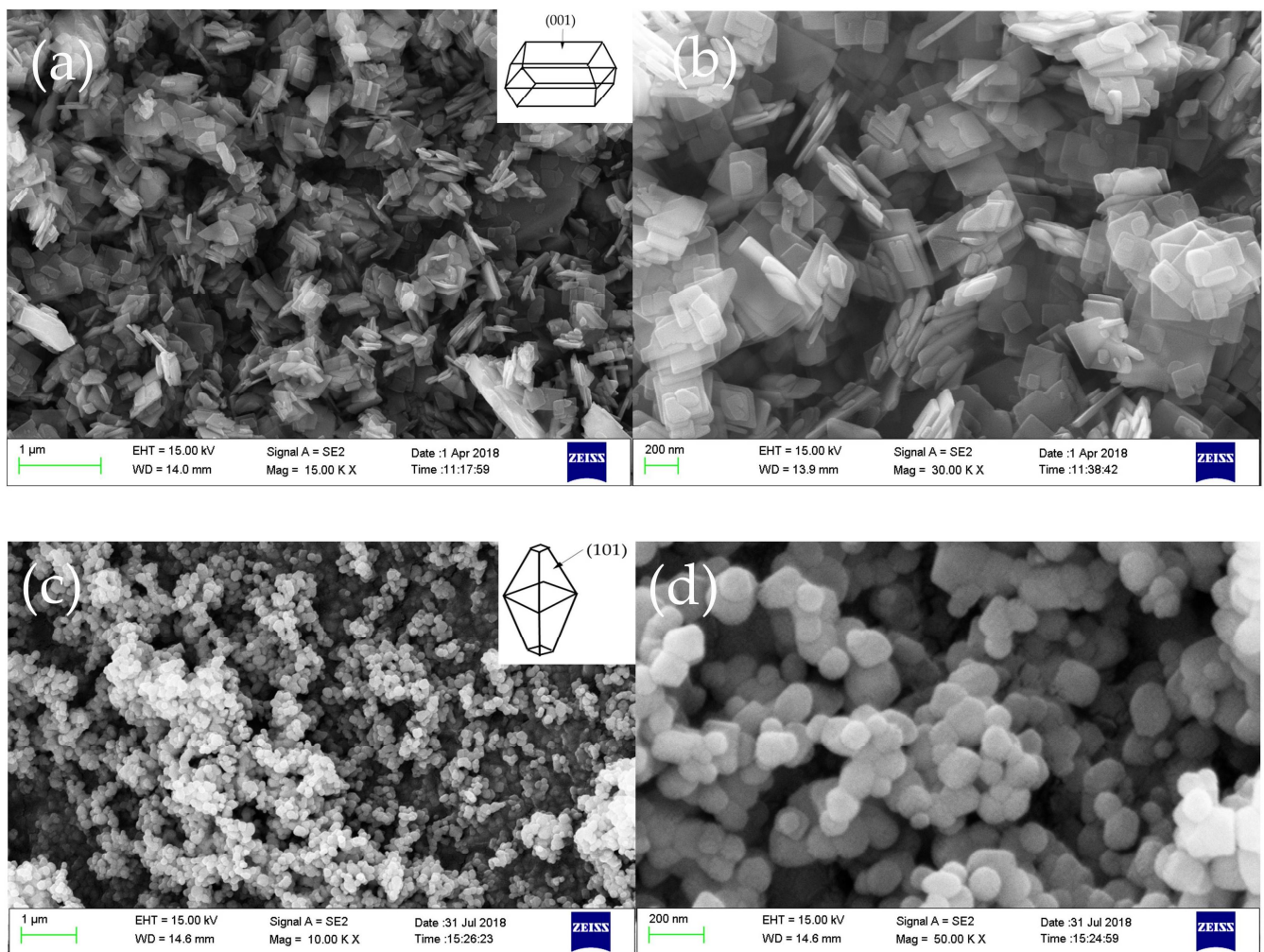
Figure 2. SEM of anatase (TiO$_2$) with exposed (001) facets (**a**,**b**) and anatase (TiO$_2$) with exposed (101) facets (**c**,**d**).

The (004) and (200) atomic planes on anatase (TiO$_2$) with exposed (001) with a lattice spacing of 0.24 nm and 0.19 nm as shown in Figure 3. This indicates that the synthesized anatase nanorods were elongated along the [001] direction [46,47]. We observed lattice fringes of about 0.35 nm on the ordinary anatase (TiO$_2$) with exposed (101) facets, indicating that the ordinary anatase (TiO$_2$) was basically composed of (101) crystal facets [48]. Among several crystal facets with relatively better activity of anatase (TiO$_2$), the (101) crystal facets have lower surface energy and better thermal stability, which has a greater advantage in the formation of crystal facets. Therefore, most of the uncontrolled anatase (TiO$_2$) morphologies are basically (101) crystal facets [49]. With the addition of HCl and HF as morphology control agents in the anatase (TiO$_2$) synthesis process, crystal facets with different morphologies can be synthesized under different conditions [50].
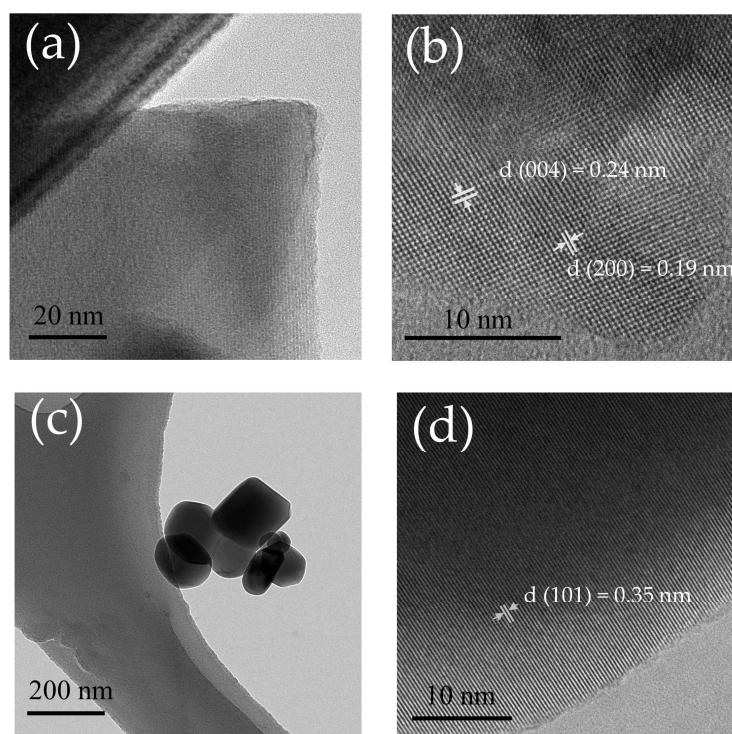
Figure 3. TEM of anatase (TiO$_2$) with exposed (001) facets (**a**,**b**) and anatase (TiO$_2$) with exposed (101) facets (**c**,**d**).

3.2. Adsorption of Glycine on Different Anatase Minerals and Influencing Factors

Amino acids are the smallest structural units that make up biological polypeptides and proteins [51]. The main chain contains both acidic carboxyl groups and basic amino groups, which can be in different states depending on the pH value of the aqueous solution. The fitting curves in Figure 4a show that glycine exists as a positive ion when the pH is <2.0, and it exists as a negative ion when the pH is >9.0 [11]. On the other hand, glycine exists as a zwitterion in the aqueous solution.

The amount of glycine absorbed on anatase (TiO$_2$) with exposed (001) facets and anatase (TiO$_2$) with exposed (101) facets under different pH conditions is shown in Figure 4b. It can be concluded that the amount of glycine absorbed on the two anatase (TiO$_2$) surfaces first increases and then decreases with a change in the pH. The adsorption of glycine molecules on the anatase (TiO$_2$) with exposed (001) facets reached a maximum at pH = 5.0 (about 4.00 mg/m^2). At pH = 6.0, the adsorption on the anatase (TiO$_2$) with exposed (101) facets reached a maximum (about 1.16 mg/m^2). Compared with the anatase (TiO$_2$) with exposed (101) facets, glycine has a better adsorption effect on the anatase (TiO$_2$) with exposed (001) facets under different pH conditions. The negatively charged glycine repelled the negatively charged anatase (TiO$_2$) on the surface when the pH of the solution was too high [52]. In earlier studies on the adsorption of small biological molecules, such as amino acids, on clay minerals also showed the best adsorption effects occurred under weakly acidic conditions [8,53].
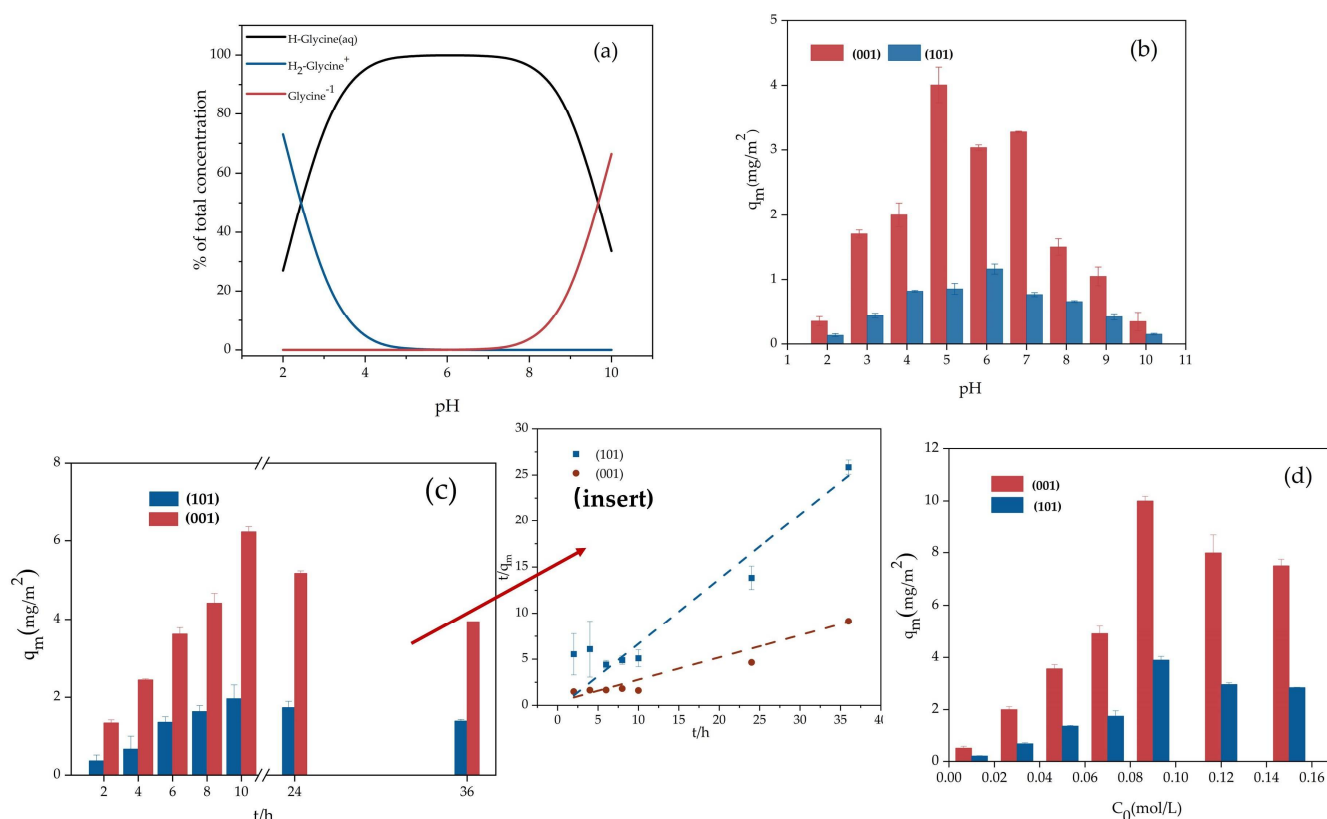
Figure 4. (**a**) The states of existence of glycine in different pH aqueous solutions. (**b**) Amount of glycine adsorbed on two kinds of anatase (TiO$_2$) at different initial pH levels. (**c**) Amount of glycine adsorbed on two kinds of anatase (TiO$_2$) for different adsorption times (insert: pseudo−secon−order kinetic fitting). (**d**) Amount of glycine adsorbed on two kinds of anatase (TiO$_2$) at different initial concentrations.

The amount of glycine adsorbed on the two kinds of anatase (TiO$_2$) with different adsorption times is shown in Figure 4c. It can be concluded that the adsorption of glycine on the two kinds of anatase (TiO$_2$) reached the maximum and then gradually decreased. In addition, the adsorption of glycine on anatase (TiO$_2$) with exposed (001) facets was significantly higher than that on ordinary anatase (TiO$_2$) at different adsorption times. The fitting curves in Figure 4c (insert) show that the adsorption of glycine on the anatase (TiO$_2$) with exposed (001) facets and (101) facets are in line with pseudo−secon−order kinetics. The adsorption process of glycine was carried out in an aqueous solution. Glycine molecules have the ability to replace water molecules adsorbed on the surface of anatase (TiO$_2$) to positions with lower desorption activation energy. However, during the long-term mixed adsorption process in the solution, competition with water molecules will affect the adsorption of small glycine molecules on the surface of anatase (TiO$_2$) [54]. Therefore, in order to achieve stable adsorption of small glycine molecules on the two anatase (TiO$_2$) surfaces, the subsequent condensation experiment set t = 24 h as the mixing oscillation time.

Figure 4d shows the amount of glycine adsorbed on the two kinds of anatase (TiO$_2$) at different initial concentrations. The adsorption of small glycine molecules on the two kinds of anatase (TiO$_2$) reached the maximum adsorption at about 0.09 mol/L. Compared with the anatase (TiO$_2$) with exposed (101) facets, the anatase (TiO$_2$) with exposed (001) facets exhibited a significant adsorption effect under different initial solution concentrations. The maximum adsorption quantity of glycine on the (001) crystal facets was 10.00 mg/m^2, and the maximum adsorption capacity of the ordinary anatase (TiO$_2$) surface was 3.89 mg/m^2. When the adsorption coverage of the adsorbed substance on the anatase (TiO$_2$) with exposed (001) facets surface increased, the surface molecules produced repulsion and then

the adsorption was weakened [55]. This may be the reason why the amount of glycine molecules adsorbed in this study showed a decreasing trend at concentrations higher than 0.09 mol/L. Through the determination of the amounts adsorbed under the different concentrations described above, an initial glycine concentration of 0.09 mol/L was selected as the initial adsorption concentration in the subsequent experiments.

3.3. Spectroscopic Analysis of the Adsorption of Glycine on Different Anatase Minerals

3.3.1. Raman Spectroscopy Analysis

Glycine has three different crystal phases, namely α-, β-, and γ-, and the thermodynamic stability is γ > α > β [56]. After the interaction of glycine with the two minerals, the peak disappeared at a wavenumber around 1341 cm^{-1}, which corresponds to the CH_2 wagging mode of blank glycine (Figure 5a) [57]. Simultaneously, the peak of blank glycine around 1439 cm^{-1} corresponds to the CH_2 wagging mode, which shifted to higher wavenumbers. The peak around 1584 cm^{-1} shifted to lower wavenumbers, corresponding to the CH_2 wagging mode of blank glycine. Figure 5b also shows the disappearance or movement of peaks at particular wavenumbers. According to Ensieh et al. [58], who reported on the crystalline phase of glycine, it can be concluded that the blank glycine in Figure 5 is thermodynamically stable γ-glycine. These changes also indicate that anatase (TiO_2) can effectively induce and activate glycine, and γ-glycine is converted into the thermodynamically unstable β-glycine after reacting with the two kinds of anatase (TiO_2).
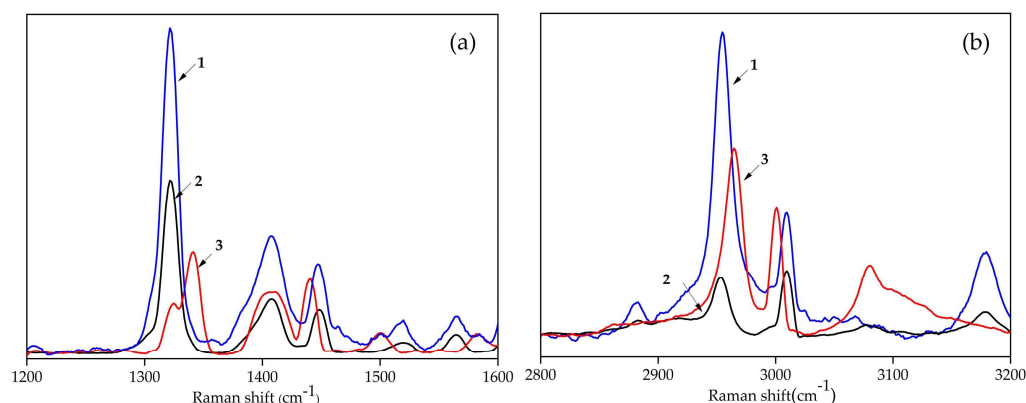

Figure 5. The Raman spectra of glycine before and after absorption on two kinds of anatase (TiO_2). (**a**) 1200−1600 cm^{-1}; (**b**) 2800−3200 cm^{-1}. 1: Glycine adsorbed on anatase (TiO_2) with exposed (101) facets; 2: glycine adsorbed on anatase (TiO_2) with exposed (001) facets; 3: blank glycine.

3.3.2. XPS Analysis

Figure 6a shows the XPS spectra of Ti atoms of the two kinds of anatase (TiO_2) before and after the adsorption of glycine. The Ti atom of anatase (TiO_2) has two chemical states: $Ti(2p_{3/2})$ and $Ti(2p_{1/2})$ [59]. Compared with anatase (TiO_2) before glycine adsorption, the binding energies of Ti ($2p_{1/2}$) and Ti ($2p_{3/2}$) reduced by about 0.24 eV after the adsorption of glycine. The intensity of the absorption peaks at the two binding energies of Ti 2p showed a uniform attenuation after the two kinds of anatase (TiO_2) adsorbed glycine. The results show that both types of anatase (TiO_2) may form Ti-O bonds with glycine [34]. The amino acid coverage rate was calculated by Fleming et al. [59] in a study of the adsorption reaction of amino acids on the surface of rutile. Combining those findings with the data of this study, we can conclude that the surface coverage of glycine on the (001) crystal facets is 0.68 and the surface coverage of anatase (TiO_2) with exposed (101) facets is 0.56. It is suggested that anatase (TiO_2) with exposed (001) crystal facets has a better adsorption effect.
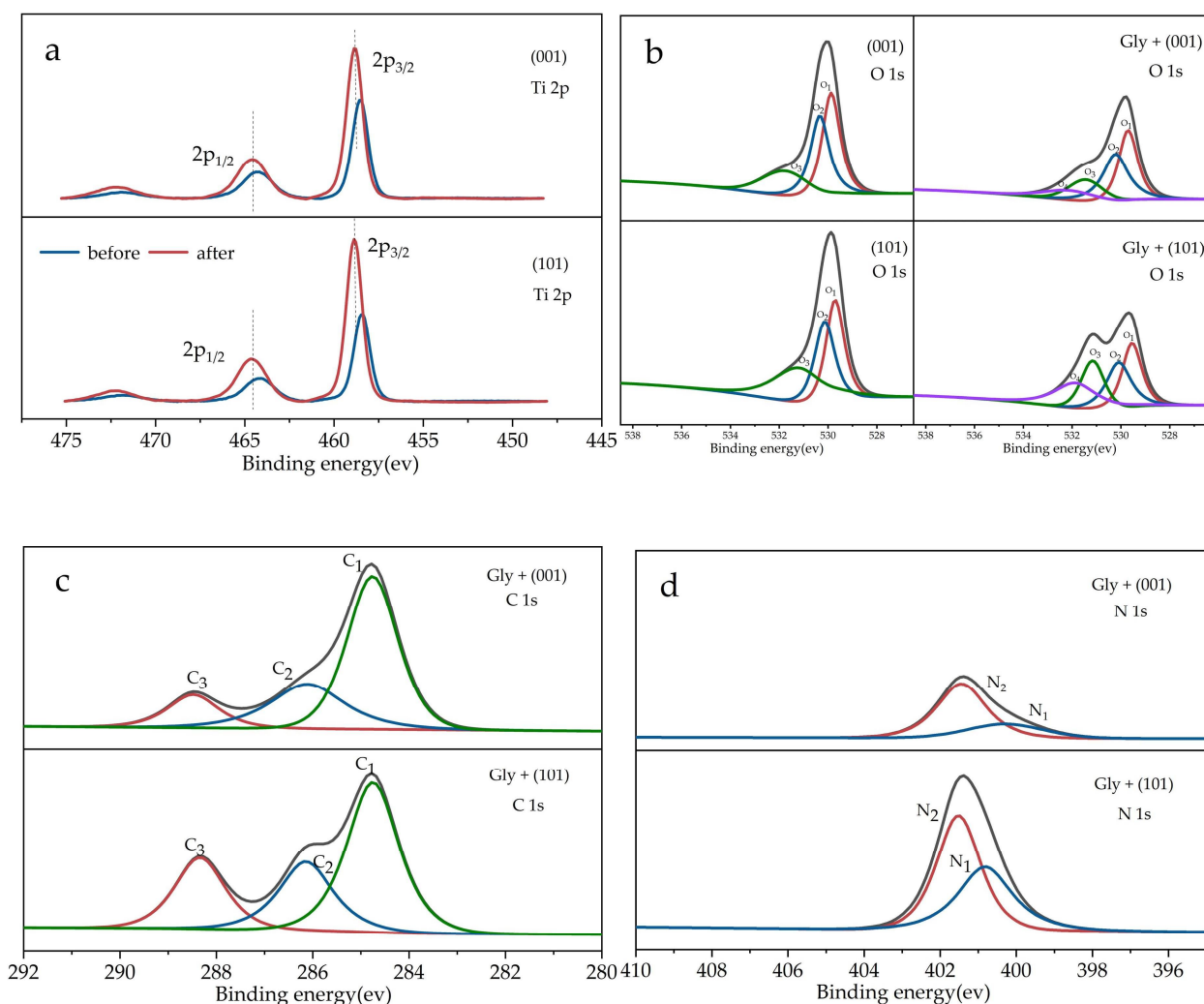
Figure 6. X-ray photoelectron spectrum curve. (**a**) XPS spectra of Ti atoms of two kinds of anatase (TiO_2) before and after the adsorption of glycine. (**b**) O 1s spectrum of two kinds of anatase (TiO_2) before and after the adsorption of glycine. (**c**) C 1s spectrum of two kinds of anatase (TiO_2) after the adsorption of glycine. (**d**): N 1s spectrum of two kinds of anatase (TiO_2) after the adsorption of glycine.

Before adsorption, O 1s is decomposed into three peaks: O_1, O_2, and O_3 (Figure 6b). The signal peaks of O_1 and O_2 are derived from Ti-O on the anatase (TiO_2) substrate and hydroxyl oxygen on the surface of anatase (TiO_2) [60]. The O_3 signal is derived from the carbon–oxygen double bond or HCO_3^- [61,62]. After glycine was mixed with and adsorbed by the anatase (TiO_2) with (001) facets, the signal peaks generated by the oxygen at each position of the anatase (TiO_2) reduced significantly, and the signal peak caused by glycine COO^- around 532.13 eV can be clearly observed. This position is similar to the adsorption of a series of amino acids on metals and the adsorption of homocysteine on titanium dioxide films [62,63]. The C 1s spectrum can be decomposed into three different chemical states, C_1, C_2, and C_3, which are $(CH_2)_n$, C=O, COO^-, or absorption signals caused by dissociated carbonate (Figure 6c) [64]. There are C signals before and after the adsorption of anatase (TiO_2), which may be caused by unremoved trace reaction raw materials and other pollutants during sample preparation or processing, which caused slight contamination of the sample [65]. In the N 1s spectrum of glycine after adsorption, the N 1s signal is decomposed into two peaks: N_1 is the amino group of the neutral glycine molecule, and N_2 comes from the protonated NH_3^+ group after dissociation in the solution [66]. This

shows that during the adsorption process, the adsorption of glycine mainly has two forms: zwitterion and dissociation.

Figure 6 shows that the anatase (TiO$_2$) with exposed (101) facets also has a good adsorption of glycine. The adsorption of glycine on anatase (TiO$_2$) with exposed (101) facets, it significantly increased to the C$_3$ signal of COO$^-$ in the spectrum of C 1s and the signal peaks of O$_3$ and O$_4$ in the spectrum of O 1s. This shows that the adsorption of glycine on the surface of ordinary anatase (TiO$_2$) is mainly in the form of zwitterions, while the adsorption on the anatase (TiO$_2$) with exposed (001) facets is mainly in the form of dissociation [34]. Meanwhile, compared with the anatase (TiO$_2$) with exposed (001) facets, the N$_1$ signal peak (NH$_3^+$) in the spectrum of N 1s is enhanced, and the N$_2$ signal peak (NH$_2$) is weakened. This relative intensity change has confirmed this point.

3.4. Analysis of the Adsorption Mechanism Based on a Molecular Simulation

Material Studio software was used to simulate the adsorption of zwitterions, dissociated positive ions, and dissociated negative ions of glycine on the surfaces of the two types of anatase (TiO$_2$). Ordinary anatase (TiO$_2$) is basically composed of (101) facets with higher surface energy. Therefore, in the simulation study of molecular and crystal surface adsorption, the (101) surface was constructed to replace ordinary anatase (TiO$_2$) for the analysis. Figure 7a–c shows the three dissociation states of glycine's dissociated positive ions, zwitterionic, and dissociated negative ions. Figure 7d,e shows the (001) and (101) facets of the complete anatase (TiO$_2$), which were constructed by using Material Studio software. It is characterized by the presence of fivefold-coordinated Ti ions (Ti$_{5c}$), twofold-coordinated bridged oxygen O ions (O$_{2c}$), threefold-coordinated O atoms (O$_{3c}$), and sixfold-coordinated Ti atoms (Ti$_{6c}$) [40]. The terminating atoms are twofold-coordinated O ions and fivefold-coordinated Ti ions, which are the most stable of the surface structure. However, there are only fivefold-coordinated Ti ions (Ti$_{5c}$) and twofold-coordinated bridged oxygen O ions (O$_{2c}$) on the anatase (TiO$_2$) with exposed (001) facets [67].
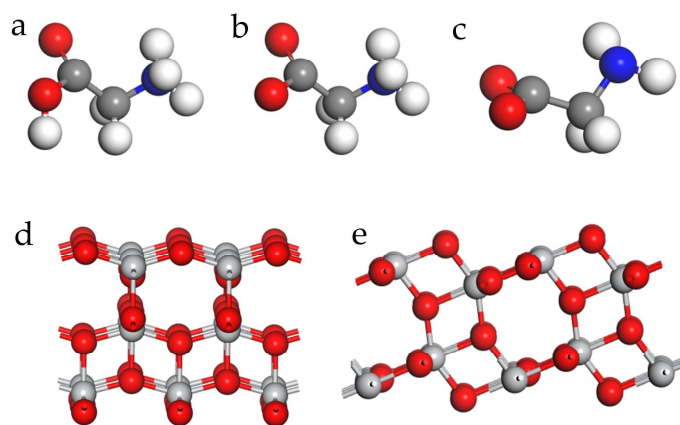

Figure 7. Three dissociation states of glycine and two kinds of anatase TiO$_2$: (**a**) positive dissociated Gly ions; (**b**) ZW zwitterions; (**c**) negative dissociated glycine ions; (**d**) anatase (TiO$_2$) with exposed (001) facets; (**e**) anatase (TiO$_2$) with exposed (101) facets.

Glycine mainly exists in the form of positive dissociated glycine ions (HCOO–CH$_2$–NH$_3^+$), negative dissociated glycine ions (NH$_2$–CH–COO$^-$) and glycine zwitterions ($^-$OOC–CH$_2$–NH$_3^+$) [68]. Figure 8 shows the adsorption model of the main chain carboxyl and amino groups of glycine in the dissociated state and the zwitterionic state in anatase (TiO$_2$) with exposed (001) facets. Schmidt et al. [65] studied the amino acids on the surface of titanium dioxide in an aqueous solution and showed that the adsorption of amino acids on the surface of titanium dioxide occurs preferentially in acidic solutions and shows specific adsorption with Ti atoms on the surface. The groups involved in the adsorption process mainly include the main chain amino and carboxyl groups shared by all amino

acids. Table 1 shows the calculated adsorption energy of glycine groups in each state on the anatase (TiO_2) with exposed (001) and (101) facets. Through simulations, we have found that when glycine forms a bridge structure with two Ti atoms on the surface through COO^- in the form of zwitterions, as shown in Figure 8a, and the calculated adsorption energy is about 26 kJ/mol. When glycine forms a bridging structure with Ti atoms at the (001) facets, this is coordinated through –COOH group in the form of positive disassociating ions, as shown in Figure 8b, and the calculated adsorption energy is 97.34 kJ/mol. Under weakly acidic conditions, the adsorption energy of the amphoteric ion form is much lower than that of the dissociation form of positive ions, indicating that glycine may be mainly adsorbed on anatase (TiO_2) with exposed (001) facets in the form of positive dissociated ions. When the positive dissociated glycine ions and the zwitterion carboxyl is adsorbed to the Ti–O group on the surface, the Ti-O (glycine carboxyl oxygen) bond length is about 2.0 Å to 2.2 Å. In addition, –COOH, which is a dissociated positive ion, is dissociated during surface adsorption, –COO^- combines with two Ti atoms connected by bridging oxygen, and the dissociated H atom combines with the surface bridging oxygen to form –OH. This adsorption method is consistent with Fleming et al. [59].
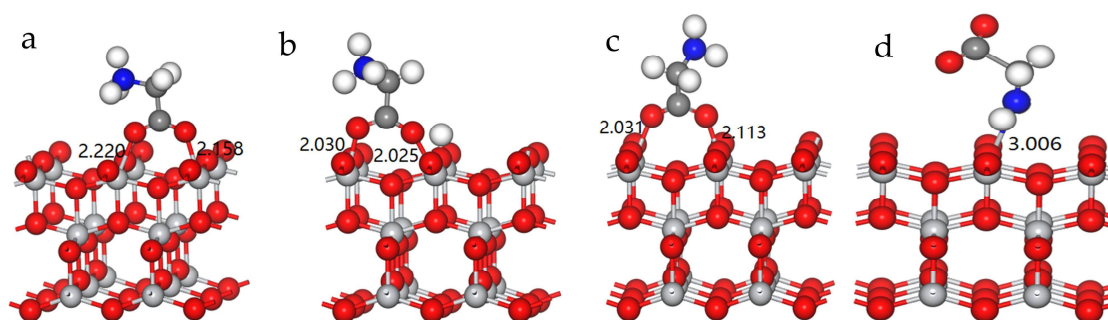

Figure 8. Adsorption model of three dissociated forms of glycine on anatase (TiO_2) with exposed (001) facets. (**a**) zwitterionic COO^-; (**b**) positive dissociated ions of –COOH; (**c**) negative dissociated ions of –COO^-; (**d**) negative dissociated ions of –NH_2.

Table 1. Adsorption energy of different dissociated forms of glycine on the two kinds of anatase (TiO_2) (unit: kJ/mol).

Adsorption Type	Energy (001)	Energy (101)
$Ti–O + {}^-OOC–CH_2–NH_3^+$	25.78	120.52
$Ti–O + HCOO–CH_2–NH_3^+$	97.34	37.49
$Ti–O + {}^-OOC–CH_2–NH_2$	124.93	45.71
$Ti–O + NH_2–CH_2–COO^-$	41.11	117.57

Figure 8c,d shows the adsorption of the –COO^- and NH_2 groups in the form of negative dissociated ions of glycine on the (001) surface. The bond lengths of the Ti–O bond and the Ti–N bond formed by the interaction of the –COO^- group and the NH_2 group with the surface Ti atom are about 2.1 Å and 3.0 Å. The adsorption energy of the bridged structure formed by the COO^- group of glycine and the Ti atom connected by the bridging oxygen is 124.93 kJ/mol, which is greater than that of the interaction between -COOH with the surface Ti atoms [36]. However, the calculated adsorption energy of the NH_2 group is 41.11 kJ/mol, indicating that adsorption between the carboxyl end and the surface may be the main type of adsorption during the adsorption process. In a solution, as the pH increases, the glycine anions will repel the negatively charged α–TiO_2 surface [52]. According to this analysis, under the weakly acid conditions in this study, glycine is mainly adsorbed by dissociated molecules on the (001) facets, and zwitterions are auxiliary [69].

Figure 9 shows the adsorption model of glycine zwitterions and the dissociated forms on the anatase (TiO_2) with exposed (101) facets. The two Ti atoms which are connected by

bridging oxygen on the (101) crystal facets were connected to glycine by bridging from the zwitterion carboxyl end, for which the calculated adsorption energy is 120.52 kJ/mol. The positive and negative dissociated glycine ions are adsorbed to the (101) facets through the bridging adsorption configuration of the carboxyl group, and the adsorption energy is 37.49 kJ/mol and 45.71 kJ/mol, respectively. A comparison of the adsorption energy of various structures suggests that the adsorption of glycine on the anatase (TiO_2) with exposed (101) facets in this study may be mainly zwitterionic, which is consistent with the results measured by XPS. Figure 9d shows the adsorption model of glycine anion NH_2 and Ti atoms on the anatase (TiO_2) with exposed (101) facets, and the adsorption energy is 117.57 kJ/mol According to the research of Ojamäe et al. [24], factors such as the plane wave cutoff energy, the number of structural crystal facets, and the calculation conditions have a certain influence on the final energy result. The cutoff energy of the plane wave in this study was 300 eV, which is enough to make the settlement result achieve a good convergence effect. The reason for the difference from the calculation in this study may be the number of structural atomic layers and the calculation conditions. Bates et al. [70] used the DFT calculation method to study the adsorption mode of formic acid on the surface of TiO_2, and found that the adsorption energy of monodentate adsorption of formic acid was 187 kJ/mol.
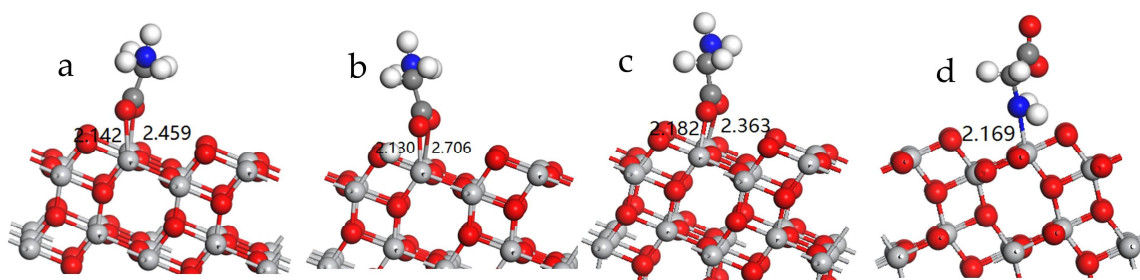

Figure 9. Adsorption model of three dissociated forms of glycine on anatase (TiO_2) with (101) facets: (**a**) zwitterionic –COO$^-$; (**b**) positive dissociated ions of –COOH; (**c**) negative dissociated ions of –COO$^-$; (**d**) negative dissociated ions of –NH$_2$.

In summary, the adsorption forms of glycine on the two anatase (TiO_2) surfaces in this study are mainly zwitterions and dissociations. There are two configurations of adsorption to the anatase (TiO_2) surface. One is by forming a bridge structure between the carboxyl group and two Ti atoms which are connected by the surface bridging oxygen; the other involves the amino group forming a bond with the surface Ti atom [71]. The calculated adsorption energies of glycine on the two types of anatase (TiO_2) are different, which resulted in a difference in the adsorption of glycine under the same conditions. On the anatase (TiO_2) with exposed (001) facets, the adsorption is mainly in the form of dissociation, and on the ordinary anatase (TiO_2), the adsorption is mainly in the form of zwitterions.

4. Conclusions

The anatase (TiO_2) which was synthesized by a hydrothermal method was mainly composed of (001) crystal facets. The ordinary anatase (TiO_2) was mainly composed of (101) crystal facets. The anatase (TiO_2) with exposed (001) facets had micro-nano flaky particles. Compared with the ordinary anatase (TiO_2), it had a better anatase crystal form and a more complete crystal structure.

The adsorption of glycine on the surfaces of the two kinds of anatase (TiO_2) showed that both anatase (TiO_2) has an adsorption effect on glycine, and the adsorption effect of the anatase (TiO_2) with (001) facets was better. The initial solution pH, concentration, and adsorption time were the main factors affecting the adsorption of glycine on the surfaces of the two kinds of anatase (TiO_2). Under optimal conditions (pH 5 to 6, an adsorption time of 24 h, and an initial concentration of 0.09 mol/L), the amount of glycine adsorbed on anatase (TiO_2) with exposed (001) facets may reach 10 mg/m^2. The anatase (TiO_2) with exposed

(001) facets and the ordinary anatase (TiO$_2$) showed better adsorption of glycine under weakly acidic conditions, which is in line with the environmental pH that was beneficial to the formation of life on the early Earth. In the early Earth environment, semiconductor minerals can adsorb and concentrate highly diluted small biological molecules such as clay minerals.

According to a combination of various characterizations and simulation calculations, the adsorption of glycine on the surface of anatase (TiO$_2$) with exposed (001) facets and anatase (TiO$_2$) with exposed (101) facets is mainly in the form of dissociation and zwitterions, respectively. The adsorption of glycine to the surface of anatase (TiO$_2$) is through two configurations: one is the Ti atom forming a bridge structure with the carboxyl group on the surface, and the other is the amino group forming a bond with the Ti atom on the surface; however, the former dominates. The calculated adsorption energies of glycine on the two types of anatase (TiO$_2$) are different, resulting in a difference in the adsorption of glycine under the same conditions. On the anatase (TiO$_2$) with exposed (001) facets, the adsorption is mainly in the form of dissociation, and on the anatase (TiO$_2$) with exposed (101) facets, the adsorption is mainly in the form of zwitterions. With the same specific surface area, the anatase (TiO$_2$) with exposed (001) facets has lower glycine adsorption energy than ordinary anatase (TiO$_2$).

The results of this research can provide a reference for the further study of the role of semiconductor minerals in the adsorption and polymerization of small biomolecules in the origin of life.

References

1. Greiner, E.; Kumar, K.; Sumit, M.; Giuffre, A.; Zhao, W.; Pedersen, J.; Sahai, N. Adsorption of L-glutamic acid and L-aspartic acid to γ-Al$_2$O$_3$. *GeCoA* **2014**, *133*, 142–155. [CrossRef]
2. Zhu, C.; Wang, Q.; Huang, X.X.; Yun, J.; Hu, Q.; Yang, G. Adsorption of amino acids at clay surfaces and implication for biochemical reactions: Role and impact of surface charges. *Colloids Surf. B Biointerfaces* **2019**, *183*, 110458. [CrossRef] [PubMed]
3. Gallori, E.; Benedetti, E.; Bramanti, E.; Franchi, M.; Orioli, P.L.; Vettori, C. Studies on the adsorption and binding of nucleic acids on clay minerals. *Orig. Life Evol. Biosph.* **1996**, *26*, 254–255. [CrossRef]
4. Benetoli, L.O.; de Souza, C.M.; da Silva, K.L.; de Souza, I.G., Jr.; de Santana, H.; Paesano, A., Jr.; da Costa, A.C.; Zaia, C.T.; Zaia, D.A. Amino acid interaction with and adsorption on clays: FT-IR and Mossbauer spectroscopy and X-ray diffractometry investigations. *Orig. Life Evol. Biosph.* **2007**, *37*, 479–493. [CrossRef]
5. Kitadai, N.; Yokoyama, T.; Nakashima, S. In situ ATR-IR investigation of L-lysine adsorption on montmorillonite. *J. Colloid Interface Sci.* **2009**, *338*, 395–401. [CrossRef] [PubMed]
6. de Castro Silva, F.; Lima, L.C.B.; Silva-Filho, E.C.; Fonseca, M.G.; Lambert, J.-F.; Jaber, M. A comparative study of alanine adsorption and condensation to peptides in two clay minerals. *Appl. Clay Sci.* **2020**, *192*, 105617. [CrossRef]
7. Jaber, M.; Georgelin, T.; Bazzi, H.; Costa-Torro, F.; Lambert, J.-F.; Bolbach, G.; Clodic, G. Selectivities in Adsorption and Peptidic Condensation in the (Arginine and Glutamic Acid)/Montmorillonite Clay System. *J. Phys. Chem. C* **2014**, *118*, 25447–25455. [CrossRef]
8. Ramos, M.E.; Huertas, F.J. Adsorption of glycine on montmorillonite in aqueous solutions. *Appl. Clay Sci.* **2013**, *80–81*, 10–17. [CrossRef]
9. Ikhsan, J.; Johnson, B.B.; Wells, J.D.; Angove, M.J. Adsorption of aspartic acid on kaolinite. *J. Colloid Interface Sci.* **2004**, *273*, 1–5. [CrossRef] [PubMed]
10. Porter, T.L.; Eastman, M.P.; Hagerman, M.E.; Price, L.B.; Shand, R.F. Site-Specific Prebiotic Oligomerization Reactions of Glycine on the Surface of Hectorite. *J. Mol. Evol.* **1998**, *47*, 373–377. [CrossRef]

11. Lambert, J.-F.; Stievano, L.; Lopes, I.; Gharsallah, M.; Piao, L. The fate of amino acids adsorbed on mineral matter. *Planet. Space Sci.* **2009**, *57*, 460–467. [CrossRef]

12. Noren, K.; Loring, J.S.; Persson, P. Adsorption of alpha amino acids at the water/goethite interface. *J. Colloid Interface Sci.* **2008**, *319*, 416–428. [CrossRef]

13. Lambert, J.F. Adsorption and polymerization of amino acids on mineral surfaces: A review. *Orig. Life Evol. Biosph.* **2008**, *38*, 211–242. [CrossRef] [PubMed]

14. Takano, Y.; Horiuchi, T.; Marumo, K.; Nakashima, M.; Urabe, T.; Kobayashi, K. Vertical distribution of amino acids and chiral ratios in deep sea hydrothermal sub-vents of the Suiyo Seamount, Izu-Bonin Arc, Pacific Ocean. *Org. Geochem.* **2004**, *35*, 1105–1120. [CrossRef]

15. Tentorio, A.; Canova, L. Adsorption of a-amino acids on spherical TiO$_2$ particles. *Colloids Surf.* **1989**, *39*, 311–319. [CrossRef]

16. Lu, A.; Li, Y.; Jin, S. Interactions between Semiconducting Minerals and Bacteria under Light. *Elements* **2012**, *8*, 125–130. [CrossRef]

17. Jonsson, C.M.; Jonsson, C.L.; Sverjensky, D.A.; Cleaves, H.J.; Hazen, R.M. Attachment of L-glutamate to Rutile (alpha-TiO$_2$): A potentiometric, Adsorption, and Surface Complexation Study. *Langmuir* **2009**, *25*, 12127–12135. [CrossRef] [PubMed]

18. Ustunol, I.B.; Gonzalez-Pech, N.I.; Grassian, V.H. pH-dependent adsorption of alpha-amino acids, lysine, glutamic acid, serine and glycine, on TiO$_2$ nanoparticle surfaces. *J. Colloid. Interface Sci.* **2019**, *554*, 362–375. [CrossRef] [PubMed]

19. Giacomelli, C.E.; Avena, M.J.; Pauli, C.P.D. Aspartic Acid Adsorption onto TiO$_2$ Particles Surface. Experimental Data and Model Calculations. *Am. Chem. Soc. J.* **1995**, *11*, 3483–3490. [CrossRef]

20. Pászti, Z.; Guczi, L. Amino acid adsorption on hydrophilic TiO$_2$: A sum frequency generation vibrational spectroscopy study. *Vib. Spectrosc.* **2009**, *50*, 48–56. [CrossRef]

21. Roddick-Lanzilotta, A.D.; McQuillan, A.J. An in situ Infrared Spectroscopic Study of Glutamic Acid and of Aspartic Acid Adsorbed on TiO(2): Implications for the Biocompatibility of Titanium. *J. Colloid Interface Sci.* **2000**, *227*, 48–54. [CrossRef] [PubMed]

22. Rozza, R.; Ferrante, F. Computational study of water adsorption on halloysite nanotube in different pH environments. *Appl. Clay Sci.* **2020**, *190*, 105589. [CrossRef]

23. Ferrante, F.; Armata, N.; Cavallaro, G.; Lazzara, G. Adsorption Studies of Molecules on the Halloysite Surfaces: A Computational and Experimental Investigation. *J. Phys. Chem. C* **2017**, *121*, 2951–2958. [CrossRef]

24. Ojamae, L.; Aulin, C.; Pedersen, H.; Kall, P.O. IR and quantum-chemical studies of carboxylic acid and glycine adsorption on rutile TiO2 nanoparticles. *J. Colloid. Interface Sci.* **2006**, *296*, 71–78. [CrossRef] [PubMed]

25. Szieberth, D.; Maria Ferrari, A.; Dong, X. Adsorption of glycine on the anatase (101) surface: An ab initio study. *Phys. Chem. Chem. Phys.* **2010**, *12*, 11033–11040. [CrossRef] [PubMed]

26. Malik, A.; Hameed, S.; Siddiqui, M.J.; Haque, M.M.; Umar, K.; Khan, A.; Muneer, M. Electrical and Optical Properties of Nickel- and Molybdenum-Doped Titanium Dioxide Nanoparticle: Improved Performance in Dye-Sensitized Solar Cells. *J. Mater. Eng. Perform.* **2014**, *23*, 3184–3192. [CrossRef]

27. Wang, X.; Xu, H.; Nan, Y.; Sun, X.; Duan, J.; Huang, Y.; Hou, B. Research progress of TiO$_2$ photocathodic protection to metals in marine environment. *J Oceanol. Limnol.* **2020**, *38*, 1018–1044. [CrossRef]

28. Umar, K.; Haque, M.M.; Mir, N.A.; Muneer, M.; Farooqi, I.H. Titanium Dioxide-mediated Photocatalysed Mineralization of Two Selected Organic Pollutants in Aqueous Suspensions. *J. Adv. Oxid. Technol.* **2013**, *16*, 252–260. [CrossRef]

29. Liu, M.; Luo, L.; Dong, F.; Wei, H.; Nie, X.; Zhang, W.; Hu, W.; Ding, C.; Wang, P. Characteristics and mechanism of uranium photocatalytic removal enhanced by chelating hole scavenger citric acid in a TiO$_2$ suspension system. *J. Radioanal. Nucl. Chem.* **2018**, *319*, 147–158. [CrossRef]

30. Dong, Y.; Meng, F. Synthesis and photocatalytic properties of three dimensional laminated structure anatase TiO$_2$/nano-Fe0 with exposed (001) facets. *RSC Adv.* **2020**, *10*, 11823–11830. [CrossRef]

31. Dong, Y.; Meng, F. Effect of triblock copolymers on crystal growth and the photocatalytic activity of anatase TiO$_2$ single crystals. *RSC Adv.* **2020**, *10*, 32400–32408. [CrossRef] [PubMed]

32. Yang, H.G.; Sun, C.H.; Qiao, S.Z.; Zou, J.; Liu, G.; Smith, S.C.; Cheng, H.M.; Lu, G.Q. Anatase TiO$_2$ single crystals with a large percentage of reactive facets. *Nature* **2008**, *453*, 638–641. [CrossRef] [PubMed]

33. Zhang, D.; Li, G.; Yang, X.; Yu, J.C. A micrometer-size TiO$_2$ single-crystal photocatalyst with remarkable 80% level of reactive facets. *Chem. Commun.* **2009**, *29*, 4381–4383. [CrossRef]

34. Fleming, G.J.; Adib, K.; Rodriguez, J.A.; Barteau, M.A.; White, J.M.; Idriss, H. The adsorption and reactions of the amino acid proline on rutile TiO$_2$(110) surfaces. *Surf. Sci.* **2008**, *602*, 2029–2038. [CrossRef]

35. Thomas, A.G.; Flavell, W.R.; Chatwin, C.P.; Kumarasinghe, A.R.; Rayner, S.M.; Kirkham, P.F.; Tsoutsou, D.; Johal, T.K.; Patel, S. Adsorption of phenylalanine on single crystal rutile TiO$_2$(110) surface. *Surf. Sci.* **2007**, *601*, 3828–3832. [CrossRef]

36. Tonner, R. Adsorption of proline and glycine on the TiO$_2$(110) surface: A density functional theory study. *ChemPhysChem* **2010**, *11*, 1053–1061. [CrossRef]

37. YazdanYar, A.; Aschauer, U.; Bowen, P. Adsorption Free Energy of Single Amino Acids at the Rutile (110)/Water Interface Studied by Well-Tempered Metadynamics. *J. Phys. Chem. C* **2018**, *122*, 11355–11363. [CrossRef]

38. Gong, X.Q.; Selloni, A.; Vittadini, A. Density Functional Theory Study of Formic Acid Adsorption on Anatase TiO$_2$(001): Geometries, Energetics, and Effects of Coverage, Hydration, and Reconstruction. *J. Phys. Chem. B* **2006**, *110*, 2804–2811. [CrossRef]

39. Feng, S.; Yang, J.; Zhu, H.; Liu, M.; Zhang, J.; Wu, J.; Wan, J. Synthesis of Single Crystalline Anatase TiO₂ (001) Tetragonal Nanosheet-Array Films on Fluorine-Doped Tin Oxide Substrate. *J. Am. Ceram. Soc.* **2011**, *94*, 310–315. [CrossRef]

40. Raghunath, P.; Lin, M.C. Adsorption Configurations and Reactions of Boric acid on a TiO₂ Anatase (101) Surface. *J. Phys. Chem. C* **2008**, *112*, 8276–8287. [CrossRef]

41. Filippatos, P.P.; Soultati, A.; Kelaidis, N.; Petaroudis, C.; Alivisatou, A.A.; Drivas, C.; Kennou, S.; Agapaki, E.; Charalampidis, G.; Yusoff, A.; et al. Preparation of hydrogen, fluorine and chlorine doped and co-doped titanium dioxide photocatalysts: A theoretical and experimental approach. *Sci. Rep.* **2021**, *11*, 5700. [CrossRef] [PubMed]

42. Zhang, Y.; Shang, M.; Mi, Y.; Xia, T.; Wallenmeyer, P.; Murowchick, J.; Dong, L.; Zhang, Q.; Chen, X. Influence of the Amount of Hydrogen Fluoride on the Formation of (001)-Faceted Titanium Dioxide Nanosheets and Their Photocatalytic Hydrogen Generation Performance. *Chem. Plus Chem.* **2014**, *79*, 1159–1166. [CrossRef]

43. Zhang, Z.; Zhong, X.; Liu, S.; Li, D.; Han, M. Aminolysis route to monodisperse titania nanorods with tunable aspect ratio. *Angew. Chem. Int. Ed. Engl.* **2005**, *44*, 3466–3470. [CrossRef] [PubMed]

44. Dinh, C.T.; Nguyen, T.D.; Kleitz, F.; Do, T.O. Shape-controlled synthesis of highly crystalline titania nanocrystals. *ACS Nano* **2009**, *3*, 3737–3743. [CrossRef] [PubMed]

45. Li, H.; Zeng, Y.; Huang, T.; Piao, L.; Liu, M. Controlled Synthesis of Anatase TiO₂ Single Crystals with Dominant {001} Facets from TiO₂ Powders. *ChemPlusChem* **2012**, *77*, 1017. [CrossRef]

46. Zhao, X.; Jin, W.; Cai, J.; Ye, J.; Li, Z.; Ma, Y.; Xie, J.; Qi, L. Shape- and Size-Controlled Synthesis of Uniform Anatase TiO2 Nanocuboids Enclosed by Active {100} and {001} Facets. *Adv. Funct. Mater.* **2011**, *21*, 3554–3563. [CrossRef]

47. Yang, W.; Li, J.; Wang, Y.; Zhu, F.; Shi, W.; Wan, F.; Xu, D. A facile synthesis of anatase TiO2nanosheets-based hierarchical spheres with over 90% {001} facets for dye-sensitized solar cells. *Chem. Commun.* **2011**, *47*, 1809–1811. [CrossRef]

48. Hu, W.; Dong, F.; Zhang, J.; Liu, M.; He, H.; Wu, Y.; Yang, D.; Deng, H. Differently ordered TiO₂ nanoarrays regulated by solvent polarity, and their photocatalytic performances. *Appl. Surf. Sci.* **2018**, *442*, 298–307. [CrossRef]

49. Lazzeri, M.; Vittadini, A.; Selloni, A. Structure and energetics of stoichiometric TiO₂ anatase surfaces. *Phys. Rev. B* **2001**, *63*, 011990. [CrossRef]

50. Alivov, Y.; Fan, Z.Y. A method for fabrication of pyramid-shaped TiO₂ nanoparticles with a high {001} facet percentage. *J. Phys. Chem. C* **2009**, *113*, 12954–12957. [CrossRef]

51. Council, N.R. Protein and Amino Acids. In *Recommended Dietary Allowances*, 10th ed.; National Academies Press: Washington, DC, USA, 1989; pp. 52–77.

52. Jonsson, C.M.; Jonsson, C.L.; Estrada, C.; Sverjensky, D.A.; Cleaves, H.J.; Hazen, R.M. Adsorption of l-aspartate to rutile (α-TiO₂): Experimental and theoretical surface complexation studies. *Geochim. Cosmochim. Acta* **2010**, *74*, 2356–2367. [CrossRef]

53. O'Connor, A.J.; Hokura, A.; Kisler, J.M.; Shimazu, S.; Stevens, G.W.; Komatsu, Y. Amino acid adsorption onto mesoporous silica molecular sieves. *Sep. Purif. Technol.* **2006**, *48*, 197–201. [CrossRef]

54. Lausmaa, J.; Löfgren, P.; Kasemo, B. Adsorption and coadsorption of water and glycine on TiO₂. *J. Biomed. Mater. Res.* **1999**, *44*, 227–242. [CrossRef]

55. Liu, H.; Zhao, M.; Lei, Y.; Pan, C.; Xiao, W. Formaldehyde on TiO₂ anatase (101): A DFT study. *Comput. Mater. Sci.* **2012**, *51*, 389–395. [CrossRef]

56. Perlovich, G.; Hansen, L.K.; Bauer-Brandl, A. The polymorphism of glycine. Thermochemical and structural aspects. *J. Therm. Anal. Calorim.* **2001**, *66*, 699–715. [CrossRef]

57. Lee, A.Y.; Lee, I.S.; Myerson, A.S. Factors Affecting the Polymorphic Outcome of Glycine Crystals Constrained on Patterned Substrates. *Chem. Eng. Technol.* **2006**, *29*, 281–285. [CrossRef]

58. Seyedhosseini, E.; Ivanov, M.; Bystrov, V.; Bdikin, I.; Zelenovskiy, P.; Shur, V.Y.; Kudryavtsev, A.; Mishina, E.D.; Sigov, A.S.; Kholkin, A.L. Growth and Nonlinear Optical Properties of β-Glycine Crystals Grown on Pt Substrates. *Cryst. Growth Des.* **2014**, *14*, 2831–2837. [CrossRef]

59. Fleming, G.J.; Adib, K.; Rodriguez, J.A.; Barteau, M.A.; Idriss, H. Proline adsorption on TiO₂(110) single crystal surface: A study by high resolution photoelectron spectroscopy. *Surf. Sci.* **2007**, *601*, 5726–5731. [CrossRef]

60. Erdem, B.; Hunsicker, R.A.; Simmons, G.W.; Sudol, E.D.; Dimonie, V.L.; El-Aasser, M.S. XPS and FTIR Surface Characterization of TiO₂ Particles Used in Polymer Encapsulation. *Langmuir* **2001**, *17*, 2664–2669. [CrossRef]

61. Zubavichus, Y.; Fuchs, O.; Weinhardt, L.; Heske, C.; Umbach, E.; Denlinger, J.D.; Grunze, M. Soft X-ray-induced decomposition of amino acids: An XPS, mass spectrometry, and NEXAFS study. *Radiat. Res.* **2004**, *161*, 346–358. [CrossRef]

62. Schmidt, M.; Steinemann, S.G. XPS studies of amino acids adsorbed on titanium dioxide surfaces. *Fresenius' J. Anal. Chem.* **1991**, *341*, 412–415. [CrossRef]

63. Zhao, X.; Zhao, R.; Yang, W.J.L. Scanning tunneling microscopy investigation of L-lysine adsorbed on Cu (001). *J. Therm. Anal. Calorim.* **2000**, *16*, 9812–9818. [CrossRef]

64. Ederer, J.; Janoš, P.; Ecorchard, P.; Tolasz, J.; Štengl, V.; Beneš, H.; Perchacz, M.; Pop-Georgievski, O. Determination of amino groups on functionalized graphene oxide for polyurethane nanomaterials: XPS quantitation vs. functional speciation. *RSC Adv.* **2017**, *7*, 12464–12473. [CrossRef]

65. Schmidt, M. X-ray photoelectron spectroscopy studies on adsorption of amino acids from aqueous solutions onto oxidised titanium surfaces. *Arch. Orthop. Trauma Surg.* **2001**, *121*, 403–410. [CrossRef] [PubMed]

66. Zubavichus, Y.; Zharnikov, M.; Yang, Y.; Fuchs, O.; Heske, C.; Umbach, E.; Tzvetkov, G.; Netzer, F.P.; Grunze, M. Surface chemistry of ultrathin films of histidine on gold as probed by high-resolution synchrotron photoemission. *J. Phys. Chem. B* **2005**, *109*, 884–891. [CrossRef] [PubMed]

67. Gong, X.Q.; Selloni, A. Reactivity of anatase TiO_2 nanoparticles: The role of the minority (001) surface. *J. Phys. Chem. B* **2005**, *109*, 19560–19562. [CrossRef]

68. Roy, R.N.; Gibbons, J.J.; Guilio LaCross, J.; Krueger, C.W. Dissociation constants of the ampholyte glycine in 50 mass% methanol-water from 5 to 55 °C, with related thermodynamic quantities. *J. Solut. Chem.* **1976**, *5*, 333–343. [CrossRef]

69. Sowmiya, M.; Senthilkumar, K. Adsorption of proline, hydroxyproline and glycine on anatase (001) surface: A first-principle study. *Theor. Chem. Acc.* **2015**, *135*, 1–8. [CrossRef]

70. Bates, S.P.; Kresse, G.; Gillan, M.J. The adsorption and dissociation of ROH molecules on TiO_2 (110). *Surf. Sci.* **1998**, *409*, 336–349. [CrossRef]

71. Langel, W.; Menken, L. Simulation of the interface between titanium oxide and amino acids in solution by first principles MD. *Surf. Sci.* **2003**, *538*, 1–9. [CrossRef]